ORGANIC LETTERS

2008
Vol. 10, No. 15
3211−3214

Modulate Photoinduced Electron Transfer Efficiency of Bipolar Dendritic Systems

Yu-Hsien Lin, Hsu-Hsuan Wu, Ken-Tsung Wong,* Cheng-Chih Hsieh, Yi-Chih Lin, and Pi-Tai Chou*

Department of Chemistry, National Taiwan University, Taipei 106, Taiwan

kenwong@ntu.edu.tw; chop@ntu.edu.tw

Received May 12, 2008

ABSTRACT

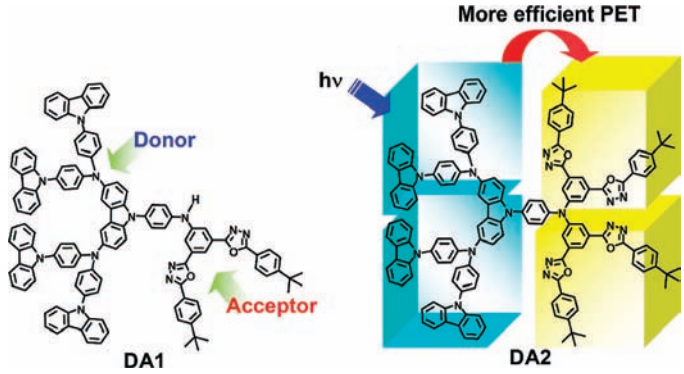

Covalent linkage of dendritic carbazole-based donors and 1,3,4-oxdiazole-based acceptors renders novel bipolar dendrimers that can efficiently facilitate the photoinduced electron transfer (PET) process. Photodynamic studies indicated that the PET rate of bipolar dendrimers DA1 and DA2 can be modulated by the number of acceptors presented in the molecule.

Photoinduced electron transfer (PET) is an essential process for solar energy conversion both in biological photosynthesis and artificial photovoltaic devices. PET occurring in molecular systems can be achieved by a covalently linked donor (D) and acceptor (A) with judicious choice of a bridging system. The rate and efficiency of electron-transfer processes can be controlled over parameters such as distance and spatial orientation between donor and acceptor. In the biological light-harvesting systems, the light-capturing chromophores are assembled into well-organized arrays which then funnel the excitation energy to the photosynthetic center in a very efficient way, triggering the charge separation for subsequent chemical reactions.[1] Inspired by this natural preorganization process, scientists have made significant endeavors for assembling molecules into an integrated system to mimic the natural photosynthesis center. In this regard, the unique molecular architectures of dendrimers provide the essential structural features for the preparation of artificial light-harvesting systems.[2] Most dendrimers enabled for efficient electron transfer are usually featured with electron-donating dendrons, which serve as antenna located at the peripheral positions of a well-defined electron-accepting core or focal point. The rate and efficiency of PET can thus be manipulated by independent modifications on the chemical structures of donor and acceptor as well as the donor's dendritic generations.[3] More recently, efficient PET processes can also be achieved in supramolecular arrays formed by noncovalent

(1) Pullerits, T.; Sundström, V. *Acc. Chem. Res.* **1996**, *29*, 381.

(2) (a) Jiang, D.-L.; Aida, T. *Nature* **1997**, *388*, 454. (b) Bar-Haim, A.; Klafter, J.; Kopelman, R. *J. Am. Chem. Soc.* **1997**, *119*, 6197. (c) Adronov, A.; Frechet, J. M. J. *Chem. Commun.* **2000**, 1701. (d) Choi, M.-S.; Aida, T.; Yamazaki, T.; Yamazaki, I. *Angew. Chem., Int. Ed.* **2001**, *40*, 3194. (e) Choi, M.-S.; Aida, T.; Yamazaki, T.; Yamazaki, I. *Chem. Eur. J.* **2002**, *8*, 2668. (f) Larsen, J.; Puntoriero, F.; Pascher, T.; McClenaghan, N.; Campagna, S.; Aakesson, E.; Sundstroem, V. *ChemPhysChem* **2007**, *8*, 2643.

10.1021/ol801096c CCC: $40.75
Published on Web 06/27/2008

interactions between electron-donating dendrimers and electron-accepting chromophores.[4]

Instead of making a funnel-like dendritic system, we have long anticipated that dendrimers incorporated with preorganized donors (donor dendron) for capturing excitation energy and with multiple electron acceptors (acceptor dendron) for trapping the photoexcited electrons could give rise to a new type of bipolar dendrimer with a more efficient PET process. In this paper, we report the synthesis, electrochemical, and phophysical properties of two novel D−A dendrimers (**DA1** and **DA2**, Scheme 1), in which the electron-donating 9-phenylcarbazole-based dendron was *covalently* hybridized with an electron-accepting 1,3,4-oxdiazole-based dendron. Carbazole and 1,3,4-oxdiazole were selected as donor and acceptor, respectively, because both of them were ubiquitously exploited in organic electronics for charge transport functions.[5] Covalent linkage of dendritic donors and acceptors creates a novel bipolar system equipped with multiple donors and acceptors that may facilitate the PET process. Photodynamic studies indicate that the PET rate of bipolar dendrimers **DA1** and **DA2** can be modulated by the number of acceptors presented in the D−A dendrimers.

Scheme 1. Synthesis of Bipolar Dendrimers **DA1** and **DA2**

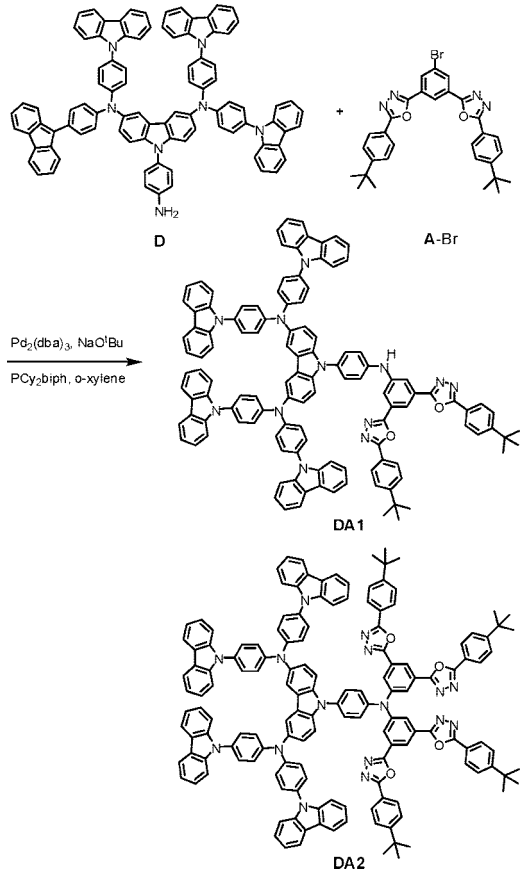

The synthesis of D−A dendrimers (**DA1** and **DA2**) is depicted in Scheme 1. The 9-phenylcarbazole-based dendron (**D**) was synthesized by our group previously through efficient C−N bond formation reactions.[6] The acceptor counterpart (**A**-Br) bearing two 1,3,4-oxadiazole moieties was synthesized according to the reported procedures.[7] The covalent hybridization of the donor and the acceptor was successfully achieved by a Pd-catalyzed C−N bond coupling reaction of 9-phenylcarbazole-based dendron **D** with 1,3,4-oxdiazole-containing bromide**A** in the presence of $Pd_2(dba)_3$ as a catalyst and 2-dicyclohexylphospine biphenyl as the ligand, yielding **DA1** and **DA2** in 30% and 67%, respectively.

Both of **DA1** and **DA2** are amorphous materials, exhibiting T_g at 237 and 250 °C, respectively, analyzed by differential scanning calorimetry (DSC), and show high thermal tolerance (T_d > 448 °C), analyzed by thermogravimetric analysis (TGA). The bipolar characters of **DA1** and **DA2** were first probed by cyclic voltammetry (CV). Both compounds exhibit two reversible one-electron oxidation potentials (**DA1**: 0.25, 0.44; **DA2**: 0.28, 0.46 V vs ferrocene/ferrocenium ion, Fc/Fc^+) followed by a multiple-electron oxidation peak centered at 0.80 V (**DA2** shown in Figure 1, **DA1** shown in Figure S-1, Supporting Information). We assigned the first two peaks to the successive oxidations of the donor's central part: 3,6-diaminocarbazole. Upon attaching to the acceptor(s), these two oxidations are slightly shifted to higher potentials as compared to those of the donor-only compound **D**, which displays the first two oxidation peaks at 0.22 and 0.42 V. The third oxidation potential (0.80 V) then was ascribed to the oxidations of peripheral carbazoles. **DA1** and **DA2** showed reversible reduction peaks at −2.47 and −2.23 V, respectively. The model compound **A** (see the Supporting Information) also displayed a reversible reduction potential at −2.42 V. Thus, the cathodic reduction couples can be unambiguously attributed to the reduction process at the phenylene ring containing 1,3,4-oxdiazole moieties. Interestingly, the **DA2** has a lower reduction potential compared to

(3) (a) Segura, J. L.; Gómez, R.; Martín, N.; Luo, C.; Swartz, A.; Guldi, D. M. *Chem. Commun.* **2001**, 707. (b) Hahn, U.; Gorka, M.; Vogtle, F.; Vicinelli, V.; Ceroni, P.; Maestri, M.; Balzani, V. *Angew. Chem., Int. Ed.* **2002**, *41*, 3595. (c) Cameron, C. S.; Gorman, C. B. *Adv. Funct. Mater.* **2002**, *12*, 17. (d) Serin, J. M.; Brousmiche, D. W.; Frechet, J. M. J. *Chem. Commun.* **2002**, 2605. (e) Thomas, K. R. J.; Thompson, A. L.; Sivakumar, A. V.; Bardeen, C. J.; Thayumanavan, S. *J. Am. Chem. Soc.* **2005**, *127*, 373. (f) Sivanandan, K.; Aathimanikandan, S. V.; Arges, C. G.; Bardeen, C. J.; Thayumanavan, S. *J. Am. Chem. Soc.* **2005**, *127*, 2020. (g) Nantalaksakul, A.; Dasari, R. R.; Ahn, T.-S.; Al-Kaysi, R.; Bardeen, C. J.; Thayumanavan, S. *Org. Lett.* **2006**, *8*, 2981.

(4) (a) Aathimanikandan, S. V.; Sandanaraj, B. S.; Arges, C. G.; Bardeen, C. J.; Thayumanavan, S. *Org. Lett.* **2005**, *7*, 2809. (b) Li, W.-S.; Kim, K. S.; Jiang, D.-L.; Tanaka, H.; Kawai, T.; Kwon, J. H.; Kim, D.; Aida, T. *J. Am. Chem. Soc.* **2006**, *128*, 10527.

(5) Carbazole: Hu, N.-X.; Xie, S.; Popovic, Z. D.; Ong, B.; Hor, A.-M. *Synth. Met.* **2000**, *111*, 421. (b) Thomas, K. R. J.; Lin, J. T.; Tao, Y.-T.; Ko, C.-W. *Adv. Mater.* **2000**, *12*, 1949. (c) Zhang, Q.; Hu, Y. F.; Cheng, Y. X.; Su, G. P.; Ma, D. G.; Wang, L. X.; Jing, X. B.; Wang, F. S. *Synth. Met.* **2003**, *137*, 1111. (d) Bugatti, V.; Concilio, S.; Iannelli, P.; Piotto, S. P.; Bellone, S.e.; Ferrara, M.; Neitzert, H. C.; Rubino, A.; Della Sala, D.; Vacca, P. *Synth. Met.* **2006**, *156*, 13. (e) Oxadiazole: Freeman, A. W.; Koene, S. C.; Malenfant, P. R. L.; Thompson, M. E.; Frechet, J. M. J. *J. Am. Chem. Soc.* **2000**, *122*, 12385. (f) Yang, X.; Jaiser, F.; Klinger, S.; Neher, D. *Appl. Phys. Lett.* **2006**, *88*, 021107/1. (g) Ichikawa, M.; Kawaguchi, T.; Kobayashi, K.; Miki, T.; Furukawa, K.; Koyama, T.; Taniguchi, Y. *J. Mater. Chem.* **2006**, *16*, 221.

(6) Wong, K.-T.; Lin, Y.-H.; Wu, H.-H.; Fungo, F. *Org. Lett.* **2007**, *9*, 4531.

(7) Kraft, A. *Liebigs Ann. Recl.* **1997**, 1463.

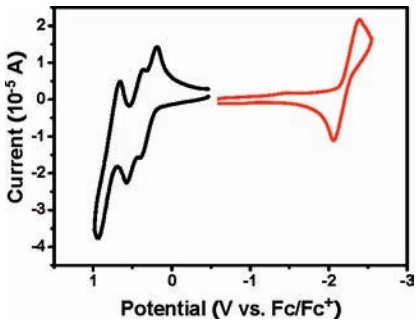

Figure 1. Cyclic voltammogram of compound **DA2** (oxidation in CH_2Cl_2 and reduction in THF).

that of **DA1**; this result points out that the LUMO energy of a D−A system can be subtly modulated by the number of acceptors attached.[8]

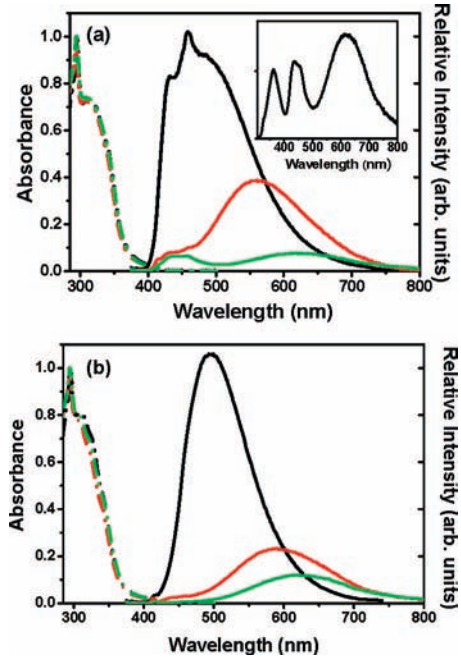

Figure 2. (a) Absorption and emission spectra of **DA1** in toluene (black), THF (red), and CH_2Cl_2 (green) where $\tau_{ex} = 380$ nm. Inset: emission spectrum of **DA1** excited at 300 nm in CH_2Cl_2. (b) Absorption and emission spectra of **DA2** in toluene (black), THF (red), and CH_2Cl_2 (green). All samples are prepared to be $\sim 10^{-5}$ M in various solvents.

Figure 2 depicts the steady-state absorption and emission spectra of **DA1** and **DA2** in various solvents. Pertinent spectroscopic and dynamic parameters are listed in Table 1. For both **DA1** and **DA2**, the absorption spectral features could be well convoluted by a linear combination of **D** and **A** chromophores, indicating a negligibly small interaction (weak

Table 1. Photophysical Properties of D−A Dendrimers **DA1** and **DA2** in Various Solvents

solvent	λ_{max} (nm)	relaxation dynamics[a] (ns)	Φ
DA1			
toluene	450	450 nm: $\tau_1 = 0.290$ (0.62)	0.147
		$\tau_2 = 10.79$ (0.38)	
		580 nm: $\tau_1 = 0.285$ (−0.33)	
		$\tau_2 = 11.36$ (0.67)	
THF	435	450 nm: $\tau_1 = 0.068$ (0.98)	0.047
		$\tau_2 = 5.65$ (0.02)	
	560	600 nm: $\tau_1 = 0.065$(−0.67)	
		$\tau_2 = 8.95$ (0.33)	
CH_2Cl_2	435	450 nm: $\tau = 0.0594$[b]	0.012
	620	600 nm: $\tau_1 = 0.0603$ (−0.36)[b]	
		$\tau_2 = 4.78$ (0.64)	
DA2			
toluene	495	450 nm: $\tau_1 = 0.263$ (0.64)	0.121
		$\tau_2 = 12.75$ (0.36)	
		580 nm: $\tau_1 = 0.250$ (−0.22)	
		$\tau_2 = 14.18$ (0.78)	
THF	590	450 nm: $\tau_1 = 0.0021$ (0.99)[b]	0.026
		$\tau_2 = 15.79$ (0.01)	
		610 nm: $\tau = 17.70$	
CH_2Cl_2	630	480 nm: $\tau_1 = 0.0014$ (0.80)[b]	0.012
		$\tau_2 = 4.02$ (0.20)	
		600 nm: $\tau_1 = 0.0016$ (−0.28)[b]	
		$\tau_2 = 4.92$ (0.72)	

[a] Data in parentheses is the fitted pre-exponential factor normalized to 1. [b] The ultrafast relaxation dynamics were measured by a femtosecond up-conversion system.

electronic coupling) between **D** and **A**, so that **D** and **A** can be treated as separated entities in the ground state. Furthermore, the absorption spectra exhibit nearly solvent polarity independence in the two D−A systems. The similar solvation effect indicates a rather small dipolar change between ground and Franck−Condon excited states. Conversely, the luminescence spectra of these D−A dendrimers show remarkable solvent-polarity dependence and reveal multiple emission in polar solvents.

As a prototypical example, **DA1** revealed a broad emission band maximized at ~450 nm in toluene (excitation at 380 nm). Upon increasing solvent polarity, the broad emission band (in toluene) gradually separated to dual emission with peak wavelength at 435 nm (F_1 band) and 560 nm (F_2 band) in e.g. THF. While the F_1 band revealed nearly solvent independence, the peak wavelenght of the F_2 band at 560 nm further red-shifted to 620 nm in CH_2Cl_2 (see Table 1). The quantum yield of the entire emission decreased from 0.15 in toluene to 0.01 in CH_2Cl_2. The entire emission originating from a common ground-state species is ascertained by the same fluorescence excitation spectra throughout the monitored emission wavelength of 450−700 nm, which are also effectively identical with the absorption spectrum. In yet another approach, the control **D** and **A** moieties exhibit solvent independent, normal Stokes shifted emission maxima at 430 and 344 nm, respectively (see Figure S-2, Supporting Information).

Similar solvent-polarity dependent emission was obtained for **DA2**. In toluene, **DA2** revealed a broad emission band with

(8) Ku, S.-Y.; Cheng, Y.-M.; Lin, X.-Y.; Hung, Y.-Y.; Pu, S.-C.; Wong, K.-T.; Chou, P.-T.; Lee, G.-H. *J. Org. Chem.* **2006**, *71*, 456.

peak wavelength at 495 nm in toluene and dual emission bands upon increasing the solvent polarity to THF and CH_2Cl_2, as shown in Figure 2. However, prominent difference can also be highlighted between **DA1** and **DA2**. For comparison, in the same solvents, the intensity ratio for F_1 versus F_2 band in **DA2** was much lower than that of **DA1**, and F_1 of **DA2** even became obscure in CH_2Cl_2. This intriguing observation can be rationalized via probing the corresponding relaxation dynamics for both **DA1** and **DA2** (vide infra).

As for the origin of the F_2 band, we have prepared **DA1** and **DA2** dendrimers in various solvents with different concentrations of 2×10^{-6}, 1×10^{-5}, and 1×10^{-4} M to examine the associated photophysical properties. As a result, the absorption spectra, the intensity ratio for F_1 versus F_2 bands and the emission profile all showed concentration independence. The results eliminate the possibility that the F_2 band originates from the aggregation effect and/or the excimer emission. These, in combination with the cascade type of HOMO/LUMO arrangement between **D** and **A** (measured by CV, see the Supporting Information), lead us to conclude the occurrence of PET between **D** and **A**, resulting in the F_2 emission (see Figure S-3, Supporting Information). Accordingly, the F_1 band can be unambiguously assigned to the normal emission of the donor moiety. It should be noted that when excitation at the shorter wavelength of 300 nm, in which the transition, in part, is also attributed to the acceptor moiety, **DA1** exhibited distinct triple emission, consisting of acceptor (~360 nm), donor (450 nm) and the charge transfer emission (620 nm) in CH_2Cl_2. The sum of emission nearly covers the entire range of visible spectrum (see inset of Figure 2a). The resulting multiple emission implies finite rate of PET process, as supported by the following reaction dynamics.

In the steady-state approach, the emission of **DA1** in toluene revealed a much broader bandwidth than that of the donor only moiety (Figure S-2, Supporting Information) in the same solvent. We thus suspect that PET is also operative on **DA1** (or **DA2**) in toluene. It is thus crucial to monitor the relaxation dynamics at different wavelength of **DA1** in toluene. As shown in Figure 3, the decay traces were drastically different at the very blue side and the red tail of the emission of **DA1** (or **DA2**) in toluene. Details of the associated photophysical parameters are listed in Table 1. The decay at 450 nm can be well fitted by two single exponential components, 290 ps and 10.79 ns. Conversely, the red side at 580 nm consists of a rise component of 285 ps and a decay of 11.36 ns. The decay of 290 ps at 450 nm, within experimental error, is consistent with the rise (285 ps) monitored at 580 nm, establishing a precursor−successor type of PET process. Furthermore, the identical decay component of ~11 ns between the two wavelength leads us to conclude the strong overlap of locally excited (F_1) and electron transfer (F_2) emission of **DA1** in toluene. Upon increasing solvent polarity, a decrease of the F_1 intensity implies a faster PET process. This viewpoint was further supported by the relaxation dynamics of F_1 band of 68 and 59 ps in THF and CH_2Cl_2, respectively (Table 1). Based on the same methodology, we then focused on the relaxation dynamics of **DA2** in toluene and also resolved a fast decay (263 ps) and another exceedingly long lifetime (12.75 ns) at short wavelength and a consistent risetime (250 ps) at longer wavelength of **DA2** (Table 1). Upon increasing the solvent polariy, PET in **DA2** is apparently more facile than that in **DA1**, as supported by the resolution of faster decay 2.1 and 1.4 ps for **DA2** (the F1 band) in THF and CH_2Cl_2, respectively. The results qualitatively fit mechanism of PET, in which the charge transfer species is further stabilized with increasing the solvent polarity, resulting in the reduction of solvent-induced barrier and hence the faster reaction rate.[9] Finally, the relatively long radiative lifetime (≫10 ns) for **DA1** and **DA2** in various solvents could be rationalized by a meta conjugation between oxdiazole and 4-(9*H*-carbazol-9-yl)benzenamino moieties. In the excited state, there exists a better communication mechanism through the meta-connectivity than in the ground state.[10] As a result, a slow charge recombination rate is expected for the charge transfer state (the F_2 band).

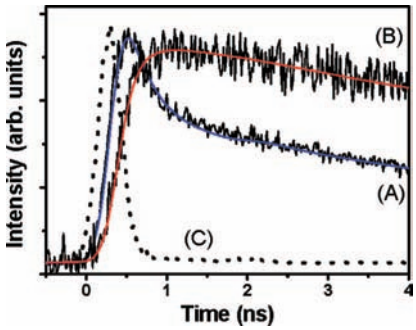

Figure 3. Relaxation dynamics of **DA1** in toluene monitored at 298 K at (A) 450 nm and (B) 580 nm. (C) The instrument response function of 380 nm. Note that with best curve fitting, the fast decay of 450 nm (290 ps) emission correlates very well with the rise of 580 nm emission (285 ps).

In conclusion, two bipolar dendritic molecules **DA1** and **DA2** composed of carbazole-based donors and a different number of 1,3,4-oxadiazole-based acceptors have been synthesized. These two dendritic systems exhibited efficient charge transfer emission, allowing us to probe the detailed electron transfer processes by spectroscopy and the associated relaxation dynamics. The photodynamics indicate that the dendrimer (**DA2**) equipped with more acceptors can efficiently facilitate the PET process. Our results may spark the demanding for a new molecular design of bipolar dendrimers use for highly efficient light-harvesting systems.

Acknowledgment. This study was supported financially by the National Science Council and Ministry of Education of Taiwan.

Supporting Information Available: Detailed experimental procedures of synthesis and photodynamics measurements; spectroscopic characterization of new compounds; cyclic voltammograms of compounds **DA1**, **D**, and **A**; photophysics of **D** and **A**. This material is available free of charge via the Internet at http://pubs.acs.org.

OL801096C

(9) Chen, K.-Y.; Hsieh, C.-C.; Cheng, Y.-M.; Lai, C.-H.; Chou, P.-T.; Chow, T.-J. *J. Phys. Chem. A* **2006**, *110*, 12136.

(10) (a) Zimmerman, H. E. *J. Am. Chem. Soc.* **1995**, *117*, 8988. (b) Thompson, A. L.; Ahn, T.-S.; Thomas, K. R. J.; Thayumanavan, S.; Martinez, T. J.; Bardeen, C. J. *J. Am. Chem. Soc.* **2005**, *127*, 16348.